Experimental Evidence for the Noninnocence of *o*-Aminothiophenolates: Coordination Chemistry of *o*-Iminothionebenzosemiquinonate(1-) π-Radicals with Ni(II), Pd(II), Pt(II)

Diran Herebian, Eberhard Bothe, Eckhard Bill, Thomas Weyhermüller, and Karl Wieghardt*

Contribution from the Max-Planck-Institut für Strahlenchemie, Stiftsstrasse 34-36, D-45470 Mülheim an der Ruhr, Germany

Abstract: The ligand 2-mercapto-3,5-di-*tert*-butylaniline, H[L^{AP}], an *o*-aminothiophenol, reacts with metal(II) salts of Ni and Pd in CH$_3$CN or C$_2$H$_5$OH in the presence of NEt$_3$ under strictly anaerobic conditions with formation of beige to yellow *cis*-[M^{II}(L^{AP})$_2$] (M = Ni (**1**), Pd (**2**)) where (L^{AP})$^{1-}$ represents the *o*-aminothiophenolate(1-) form. The crystal structure of *cis*-[Pd^{II}(L^{AP})$_2$][HN(C$_2$H$_5$)$_3$][CH$_3$CO$_2$] has been determined by X-ray crystallography. In the presence of air the same reaction produces dark blue solutions from which mixtures of the neutral complexes *trans/cis*-[M^{II}(L^{ISQ})$_2$] (M = Ni (**1a/1b**), Pd (**2a/2b**), and Pt (**3a/3b**)) have been isolated as dark blue−black solid materials. By using HPLC the mixture of **3a/3b** has been separated into pure samples of **3a** and **3b**, respectively; (L^{ISQ})$^{1-}$ represents the *o*-iminothionebenzosemiquinonate(1-) π-radical. The structures of **1a**·dmf and **3a**·CH$_2$Cl$_2$ have also been determined. All compounds are square-planar and diamagnetic. ^{1}H NMR spectroscopy established the *cis* ⇌ *trans* equilibrium of **1a/1b, 2a/2b,** and **3a/3b** in CH$_2$Cl$_2$ solution where the isomerization rate is very fast for the Ni, intermediate for the Pd, and very slow for the Pt species. It is shown that the electronic structures of **1a/1b, 2a/2b, 3a,** and **3b** are best described as diradicals with a singlet ground state. The spectro- and electrochemistries of all complexes display the usual full electron transfer series where the monocation, the neutral species, the mono- and dianions have been spectroscopically characterized. X-band EPR spectra of the monocations [**1a/1b**]$^+$ and [**3a**]$^+$ support the assignment of an oxidation-state distribution as predominantly [M^{II}(L^{ISQ})(L^{IBQ})]$^+$ where (L^{IBQ})^0 represents the *o*-iminothionequinone level. In contrast, the EPR spectra of the monoanions [**1a/1b**]$^-$ and [**3a**]$^-$ indicate an [M^{II}(L^{ISQ})(L^{AP}−H)]$^-$ distribution but with a significant contribution of the [M^I(L^{ISQ})$_2$]$^-$ resonance hybrid; (L^{AP}−H)$^{2-}$ represents the *o*-imidothiophenolato(2-) oxidation level. Analysis of the geometric features of 120 published structures of complexes containing ligands of the *o*-aminothiophenolate type show that high precision X-ray crystallography allows to discern the differing protonation and oxidation levels of these ligands. *o*-Aminothiophenolates are unequivocally shown to be noninnocent ligands; the (L^{ISQ})$^{1-}$ radical form is quite prevalent in coordination compounds and the electronic structure of a number of published complexes must be reconsidered.

Introduction

o-Diaminophenylenes,[1] *o*-catecholates[2] and, as we have shown recently, *o*-aminophenolates[3] constitute archetypal classes of redox-active, noninnocent ligands in transition metal chemistry. They exist in distinctly different oxidation and protonation levels, namely, as (i) closed-shell aromatic mono- or dianions, or (ii) closed-shell neutral *o*-quinones, or as (iii) *o*-benzosemiquinonates which are organic, open-shell radicals ($S_{rad} = 1/2$). High precision X-ray crystallography, preferably performed at

cryogenic temperatures, has shown that it is possible to clearly establish the oxidation and protonation level of such ligands in a given coordination compound.[3]

In general, the C−N (and/or C−O) bond lengths vary systematically. In *o*-diaminophenylenes two C−N single bonds are observed at ∼1.46 Å. In *o*-diiminobenzosemiquinonates these bonds are intermediate between a single and double bond at ∼1.36 Å, and in *o*-diiminoquinones two C=N double bonds at ∼1.31 Å have been found. Similar trends have been established for catecholates and *o*-aminophenolates.[3] A second structural feature is invariably observed. In the closed-shell aromatic ligands, which may be neutral, di- or monoanions depending on the level of protonation at the nitrogen substituents, the six C−C bonds of the phenyl entity are equidistant whereas the semiquinonate and quinone forms display a typical pattern of three alternating short-long-short C−C distances and three adjacent long ones.

In light of these results, it appeared to us rather surprising and unexpected that the coordination chemistry of *o*-amino-
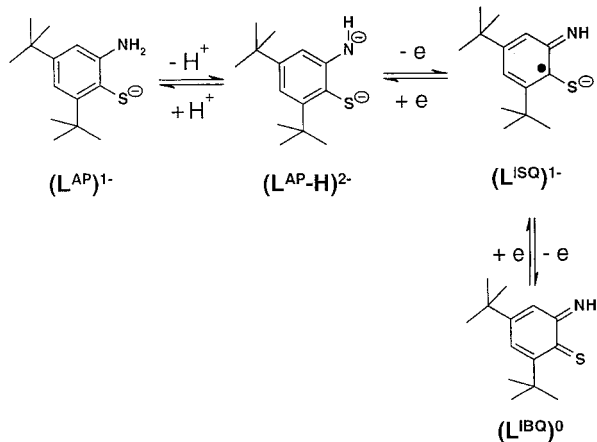
(1) (a) Carugo, O.; Djinovic', K.; Rizzi, M.; Castellani, C. B. *J. Chem. Soc., Dalton Trans.* **1991**, 1551. (b) Mederos, A.; Dominguez, S.; Hernández-Molina, R.; Sanchiz, J.; Brito, F. *Coord. Chem. Rev.* **1999**, *193−195*, 913.
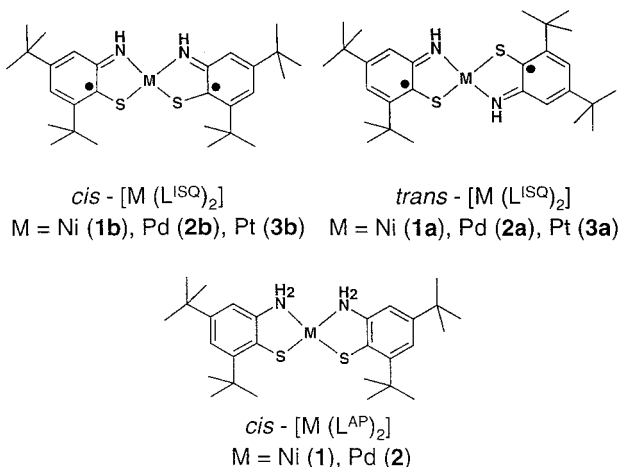(2) Pierpont, C. G.; Lange, C. W. *Prog. Inorg. Chem.* **1994**, *41*, 331.
(3) (a) Verani, C. N.; Gallert, S.; Bill, E.; Weyhermüller, T.; Wieghardt, K.; Chaudhuri, P. *Chem. Commun.* **1999**, 1747. (b) Chaudhuri, P.; Verani, C. N.; Bill, E.; Bothe, E.; Weyhermüller, T.; Wieghardt, K. *J. Am. Chem. Soc.* **2001**, *123*, 2213. (c) Chun, H.; Verani, C. N.; Chaudhuri, P.; Bothe, E.; Bill, E.; Weyhermüller, T.; Wieghardt, K. *Inorg. Chem.* **2001**, *40*, 4157. (d) Chun, H.; Weyhermüller, T.; Bill, E.; Wieghardt, K. *Angew. Chem., Int. Ed.* **2001**, *40*, 2489.

Scheme 1. Designation of Ligands and Complexes

For this purpose, we have synthesized and fully characterized a series of neutral square-planar bis(*o*-iminothionesemiquinonato)metal complexes *cis/trans*-[M(L^{ISQ})$_2$] (M = Ni, Pd, Pt) by using Sellmann's ligand 2,4-di-*tert*-butyl-6-aminothiophenol,[6] H[L^{AP}] (Scheme 1). We show that these diamagnetic neutral species contain a diamagnetic Ni^{II}, Pd^{II}, Pt^{II} (d^8) central ion and two strongly antiferromagnetically coupled, monoanionic radical ligands, (L^{ISQ})$^{1-}$. The electronic structures of these compounds are best described as diradicals with a singlet ground state. Similar complexes [ML$_2$] (M = Ni, Pd, Pt) containing the unsubstituted *o*-aminothiophenolate ligand (and oxidized forms thereof) have been described in the literature,[7−10] but only the Pt complex has been characterized by X-ray crystallography.[10]

Experimental Section

The ligand 2,4-di-*tert*-butyl-6-aminothiophenol, H[L^{AP}], has been prepared according to a published procedure.[11]

Preparation of Complexes. *cis*-[Ni^{II}(L^{AP})$_2$] (1). To a solution of the ligand H[L^{AP}] (2.3 mL, ~8.44 mmol) in dry acetonitrile (20 mL) under an argon blanketing atmosphere was added dropwise with stirring a solution of Ni(NO$_3$)$_2$·6H$_2$O (1.23 g, 4.22 mmol) in CH$_3$CN (10 mL) at room temperature. From this solution a microcrystalline beige precipitate formed within 1 h which was collected by filtration, washed with cold CH$_3$CN and dried in vacuo. Yield: 0.85 g (38%). ^{1}H NMR (500 MHz, CDCl$_3$, 298 K): δ = 1.17 (s, 18H), 1.50 (s, 18H), 5.08 (br, NH), 6.48 (d, 2H), 7.08 (d, 2H). ^{13}C{^{1}H}NMR (CDCl$_3$; 125.8 MHz): δ = 29.3; 31.3; 34.2; 36.8; 119.4; 121.9; 135.4; 143.4; 145.6; 147.7 ppm. EI-mass spectrum: m/z = 530 M$^+$. IR(KBr disk, cm^{-1}): 3191; 3250 ν(NH$_2$). Anal. Calcd for C$_{28}$H$_{44}$N$_2$S$_2$Ni: C, 63.3; H, 8.3; N, 5.3. Found: C, 62.9; H, 8.2; N, 5.1.

***trans/cis*-[Ni^{II}(L^{ISQ})$_2$] (1a/1b).** To a solution of **1** (0.50 g, 0.94 mmol) in CH$_3$CN/CH$_2$Cl$_2$ (20 mL, 1:1) was added triethylamine (0.52 mL). The solution was stirred at ambient temperature in the presence of air for 1 h. The color of the solution changed to dark blue. Evaporation of the solvent under reduced pressure afforded a microcrystalline dark blue material which was washed with cold CH$_3$CN and dried in vacuo. Single crystals of **1a**·dmf suitable for X-ray crystallography were obtained from a dimethylformamide (dmf) solution by slow evaporation. Yield: 0.47 g (95%). ^{1}H NMR (400 MHz, CDCl$_3$, 300 K): δ = 1.29 (s, 18H), 1.75 (s, 18H), 7.14 (br, 2H), 7.28 (br, 2H), 8.84 (br, NH). ^{13}C{^{1}H}NMR (62.9 MHz, CDCl$_3$): δ = 30.1; 30.7; 34.8; 36.9; 117.9; 120.3; 149.6; 150.3; 152.9; 169.0 ppm. EI-mass spectrum: m/z = 528 M$^+$, calcd 529.5. IR(KBr disk, cm^{-1}): 3298 ν(NH). Anal. Calcd for C$_{28}$H$_{42}$N$_2$S$_2$Ni: C, 63.5; H, 8.0; N, 5.3. Found: C, 63.8; H, 8.0; N, 5.3.

***cis*-[Pd^{II}(L^{AP})$_2$][NH(C$_2$H$_5$)$_3$][CH$_3$CO$_2$] (2).** To a solution of the ligand, H[L^{AP}], (1.2 mL, ~4.22 mmol) in dry ethanol (30 mL) was added 1.1 mL of NEt$_3$ and Pd(CH$_3$CO$_2$)$_2$ (0.45 g, 2 mmol). The reaction mixture was stirred at 20 °C for 10 min. The resulting yellow-brown solution was allowed to stand in an open vessel in the presence of air for 4−5 d. Yellow crystals of X-ray quality were collected by filtration. Yield: 0.36 g (24%). ^{1}H NMR (400 MHz, CD$_2$Cl$_2$, 300 K): δ = 1.10 (t, 9H), 1.24 (18 H), 1.55 (s, 18H), 1.95 (s, 3H), 2.94 (q, 6H), 6.44 (br, NH), 6.63 (d, 2H), 7.21 (d, 2H). ^{13}C{^{1}H}NMR (CD$_2$Cl$_2$, 100.61 MHz, 300 K): δ = 8.8; 29.7; 30.1; 31.5; 34.5; 37.4; 45.6; 120.8; 122.0; 122.8; 142.2; 143.8; 148.5. EI-MS: m/z = 578 [M$^+$ − (NHEt$_3$)(CH$_3$CO$_2$)]; IR(KBr disk, cm^{-1}): 3109, 3313 ν(NH$_2$). Anal. Calcd for C$_{36}$H$_{63}$N$_3$S$_2$O$_2$Pd: C, 58.4; H, 8.6; N, 5.7. Found: C, 58.2; H, 8.4; N, 5.7.

***trans/cis*-[Pd^{II}(L^{ISQ})$_2$] (2a, 2b).** To a solution of **2** (0.05 g, 0.09 mmol) in methanol (10 mL) was added a 1 M NaOCH$_3$/CH$_3$OH solution (0.18 mL). After stirring for 30 min of the solution in the presence of

thiophenolates[4] has not been described in similar terms. Despite the fact that this ligand and many organic derivatives thereof have been extensively studied in coordination compounds and more than 120 crystal structures of complexes containing at least one *o*-aminothiophenolato moiety are available in the Cambridge Crystallographic Data Base, the redox-activity of this type of ligand has rarely[5] been explicitly addressed in the past. Thus, compounds containing the *o*-iminothionebenzosemiquinonate-(1-) radical anion (Scheme 1) have not been clearly identified as such. In other words, in most of these complexes the *o*-aminothiophenolate part is believed to be redox-innocent and aromatic. This notion has recently been reemphasized,[6] where it has been stated that "*o*-aminothiophenolates behave as quite usual aminethiolate ligands".

We will show in this paper that, in fact, *o*-aminothiophenolates are noninnocent ligands. We present evidence that *o*-iminothionebenzosemiquinonate(1-) radicals, (L^{ISQ})$^{1-}$, are present in many transition metal complexes and that it is possible to develop structural and spectroscopic criteria which allow to identify the radical oxidation level unambiguously.

(4) (a) Larkworthy, L. F.; Murphy, J. M.; Phillips, D. J. *Inorg. Chem.* **1968**, *7*, 1436. (b) Holm, R. H.; O'Connor, M. J. *Prog. Inorg. Chem.* **1971**, *14*, 241.

(5) (a) Gardner, J. K.; Pariyadath, N.; Corbin, J. L.; Stiefel, E. I. *Inorg. Chem.* **1978**, *17*, 897 (see footnote 33 in this paper). (b) Ebadi, M.; Lever, A. B. P. *Inorg. Chem.* **1999**, *38*, 467.

(6) Sellmann, D.; Emig, S.; Heinemann, F. W.; Knoch, F. *Angew. Chem.* **1997**, *109*, 1250; *Angew. Chem., Int. Ed. Engl.* **1997**, *36*, 1201.

(7) Holm, R. H.; Balch, A.; Davison, A.; Maki, A.; Berry, T. *J. Am. Chem. Soc.* **1967**, *89*, 2866.

(8) Forbes, C. E.; Gold, A.; Holm, R. H. *Inorg. Chem.* **1971**, *10*, 2479.

(9) Stiefel, E. I.; Waters, J. H.; Billig, E.; Gray, H. B. *J. Am. Chem. Soc.* **1965**, *87*, 3016.

(10) Matsumoto, K.; Fukutomi, I.; Kinoshita, I.; Ooi, S. *Inorg. Chim. Acta* **1989**, *158*, 201.

(11) Sellmann, D.; Kaeppler, O. *Z. Naturforsch.* **1987**, *42b*, 1291.

Table 1. Crystallographic Data of Complexes *trans*-[Ni(L^{ISQ})$_2$]·dmf, *cis*-[Pd^{II}(L^{AP})$_2$][NH(C$_2$H$_5$)$_3$][CH$_3$CO$_2$], and *trans*-[Pt(L^{ISQ})$_2$]·CH$_2$Cl$_2$

	trans-[Ni(L^{ISQ})$_2$]·dmf	*cis*-[Pd^{II}(L^{AP})$_2$][NH(C$_2$H$_5$)$_3$][CH$_3$CO$_2$]	*trans*-[Pt(L^{ISQ})$_2$]·CH$_2$Cl$_2$
formula	C$_{31}$H$_{49}$N$_3$NiOS$_2$	C$_{36}$H$_{63}$N$_3$O$_2$PdS$_2$	C$_{29}$H$_{44}$Cl$_2$N$_2$PtS$_2$
fw, g·mol^{-1}	602.56	740.41	750.77
cryst system	monoclinic	monoclinic	orthorhombic
space group	*C*2/*c*, No. 15	*C*2/*c*, No. 15	*Pbca*, No. 61
a, Å	29.666(4)	32.301(2)	23.793(2)
b, Å	9.7420(12)	14.9776(12)	9.8009(8)
c, Å	11.614(2)	17.4278(12)	28.039(3)
β, deg	99.25(2)	105.90(2)	90
V, Å	3312.9(8)	8108.8(10)	6538.5(10)
Z	4	8	8
T, K	150(2)	100(2)	100(2)
R1^a [*I* > 2σ(*I*)]	0.0562	0.0347	0.0422
wR2^b (*I* > 2σ(*I*))	0.1243	0.0844	0.0819

^{a} R1 = Σ||F_o| − |F_c||/Σ|F_o|. ^{b} wR2 = [Σ[w(F_o^2 − F_c^2)^2]/Σ[w(F_o^2)^2]]$^{1/2}$ where w = 1/σ^2(F_o^2) + (a*P*)^2 + b*P*, *P* = (F_o^2 + 2F_c^2)/3.

air the reaction volume of the now deep-blue solution was reduced to ∼5 mL by evaporation. A violet-black microcrystalline precipitate was collected by filtration and washed twice with 2 mL of cold CH$_3$OH and dried in vacuo. Yield: 42 mg (81%). As evidenced by ^{1}H NMR the solid is a mixture of *cis*- and *trans*-[Pd^{II}(L^{ISQ})$_2$]. Due to the relatively fast *cis/trans* isomerization at 20 °C we did not attempt to separate the *cis/trans*-species. ^{1}H NMR (CD$_2$Cl$_2$, 500 MHz, 300 K) of *trans*-[Pd-(L^{ISQ})$_2$] (**2a**): δ = 1.30 (s, 18H), 1.69 (s, 18H), 7.06 (m, 4H), 8.84 (br, 2NH); *cis*-[Pd(L^{ISQ})$_2$] (**2b**): δ = 1.32 (s, 18H), 1.67 (s, 18H), 6.95 (m, 4H), 8.74 (br, 2NH). ^{13}C{^{1}H}NMR (CD$_2$Cl$_2$, 100.62 MHz, 300 K) of **2a**: δ = 30.1; 30.6; 35.0; 37.3; 119.0; 122.5; 149.7; 151.2; 156.8; 170.3; **2b**: δ = 30.3; 30.7; 35.1; 37.2; 118.7; 120.6; 149.6; 152.7; 156.7; 169.2. EI-MS: *m/z* = 576 {M$^+$}. IR(KBr disk, cm^{-1}): 3207 ν(N−H). Anal. Calcd for C$_{28}$H$_{42}$N$_2$S$_2$Pd: C, 58.3; H, 7.3; N, 4.9. Found: C, 58.1; H, 7.0; N, 5.1.

trans/cis-[Pt^{II}(L^{ISQ})$_2$] (3a, 3b). To a solution of the ligand H[L^{AP}] (0.6 mL, ∼2.11 mmol) in methanol (20 mL) was added PtCl$_2$ (0.27 g, 1.0 mmol) and triethylamine (1.1 mL). The mixture was heated at 60 °C in the presence of air for 1 h. Then the volume of the dark blue solution was reduced to ∼5 mL by evaporation under reduced pressure. As judged from the ^{1}H NMR spectrum this crude material is a 1:1 mixture of **3a/3b**. The product was purified by column chromatography (silica, methanol) and separated into the *trans*- and *cis*-isomers by HPLC on a Nucleosil-5-C18 column (Abimed Gilson 305 pump, 155 UV− vis detector operating at 210 nm), at a 4 mL/min flow rate with methanol as eluent. The first fraction contained the *trans*-isomer **3a** and the second the *cis*-isomer **3b**. The overall yield after removal of the solvent of dark-blue microcrystalline *cis*- and *trans*-isomers was ∼62%. Crystals of **3a** suitable for X-ray crystallography were grown from a CH$_2$Cl$_2$ solution by slow evaporation of the solvent. ^{1}H NMR (CD$_2$Cl$_2$, 500 MHz, 300 K) of **3a**: δ = 1.33 (s, 18H), 1.73 (s, 18H), 7.09 (d, 2H), 7.14 (d, 2H), 9.62 (br, 2NH), and of **3b**: δ = 1.35 (s, 18H), 1.70 (s, 18H), 7.12 (d, 2H), 7.27 (d, 2H), 9.57 (br, 2NH). ^{13}C{^{1}H} (CD$_2$Cl$_2$, 62.90 MHz, 300 K) of **3a**: δ = 30.1; 30.8; 34.9; 37.3; 117.7; 119.2; 123.3; 148.1; 149.7; 154.0; 166.5; and of **3b**: δ = 30.3; 30.9; 35.0; 37.2; 117.7; 119.2; 120.3; 123.3; 149.3; 152.4. EI-MS: *m/z* = 665 (M$^+$) for both isomers; IR(KBr disk, cm^{-1}): 3355 ν(N−H). Anal. of the *cis/trans* mixture: Calcd for C$_{28}$H$_{42}$N$_2$S$_2$Pt: C, 50.1; H, 6.4; N, 4.2. Found: C, 50.0; H, 6.4; N, 4.1.

X-ray Crystallographic Data Collection and Refinement of the Structures. A dark blue-black single crystal of *trans*-[Ni(L^{ISQ})$_2$]·dmf, **1a**·dmf, and a yellow crystal of *cis*-[Pd^{II}(L^{AP})$_2$][NH(C$_2$H$_5$)$_3$](CH$_3$CO$_2$), **2**, were fixed with perfluoropolyether on glass fibers and mounted on a Siemens SMART CCD diffractometer, while a dark turquoise specimen of *trans*-[Pt(L^{ISQ})$_2$]·CH$_2$Cl$_2$, **3a**, was mounted on a Nonius Kappa-CCD diffractometer. Both diffractometers were equipped with a cryogenic nitrogen cold stream (100(2) K). Graphite monochromated Mo Kα radiation (λ = 0.71073 Å) was used throughout. Crystallographic data of the compounds are listed in Table 1. Final cell constants were obtained from a least-squares fit of the setting angles of several thousand strong reflections. Intensity data were corrected for Lorentz and polarization effects. Intensity data of **1a** were corrected for absorption using the program SADABS[12] yielding a maximum and minimum transmission coefficient of 0.95 and 0.54, respectively. Face

indices and distances of crystals of **2** and **3a** were determined, and a Gaussian type absorption correction was performed using XPREP[13] yielding max/min transmission factors of 0.875/0.767 and 0.795/0.546, respectively. The Siemens ShelXTL[13] software package was used for solution, refinement, and artwork of the structures, and neutral atom scattering factors of the program were used. All structures were solved and refined by direct methods and difference Fourier techniques. Non-hydrogen atoms were refined anisotropically, while hydrogen atoms bound to carbon were placed at calculated positions and refined as riding atoms with isotropic displacement parameters. Hydrogen atoms bound to nitrogen donors were readily located from the difference map, and their position was allowed to refine without restrictions.

Physical Measurements. Equipment used and simulation procedures are the same as described in refs 3b and 3c.

Results

Syntheses. The preparation of complexes shown in Scheme 1 is straightforward and follows published procedures. The reaction of the free ligand, H[L^{AP}], with an appropriate metal salt, e.g. Ni(NO$_3$)$_2$·6H$_2$O or Pd(CH$_3$CO$_2$)$_2$, in the ratio 2:1 and two equivalents of triethylamine in acetonitrile or ethanol under strictly anaerobic conditions yields the air-sensitive, beige to yellow neutral complexes *cis*-[M^{II}(L^{AP})$_2$] (M = Ni (**1**), Pd (**2**)). Yellow single crystals of [**2**][NHEt$_3$][CH$_3$CO$_2$] were grown from an ethanol solution containing [NHEt$_3$][CH$_3$CO$_2$].

Similarly, the reaction of the ligand H[L^{AP}] and a suitable metal salt (2:1) in CH$_2$Cl$_2$/CH$_3$CN or methanol, to which four equivalents of NEt$_3$ had been added, produced in the presence of air deep blue-violet solutions, from which mixtures of solid *cis/trans*-[M(L^{ISQ})$_2$] complexes were obtained upon evaporation of the solvent. The following deep blue-black neutral complexes have been isolated: *trans/cis*-[Ni^{II}(L^{ISQ})$_2$] (**1a**, **1b**), *trans-/cis*-[Pd^{II}(L^{ISQ})$_2$] (**2a**, **2b**), *trans/cis*-[Pt^{II}(L^{ISQ})$_2$] (**3a**, **3b**). All complexes have been characterized by EI-mass spectroscopy, elemental analyses and infrared spectroscopy (see Experimental Section). All complexes are diamagnetic at ambient temperature (S = 0).

It has been possible to separate the *trans*- and *cis*-isomers of a crude solid mixture of **3a/3b** as was obtained from the primary reaction mixture by using high-pressure liquid chromatography (see Experimental Section). This proved not to be possible for mixtures of **1a/1b** and **2a/2b** because the *cis* ⇌ *trans* isomerization rate in solution is fast on the time scale of an HPLC experiment (see below).

Crystal Structure Determinations. High precision molecular structures were obtained by single-crystal X-ray crystallography of **1a**, **2**, and **3a**; Figure 1 shows the structures of neutral

(12) Sheldrick, G. M. *SADABS*; University of Göttingen: Germany, 1994.
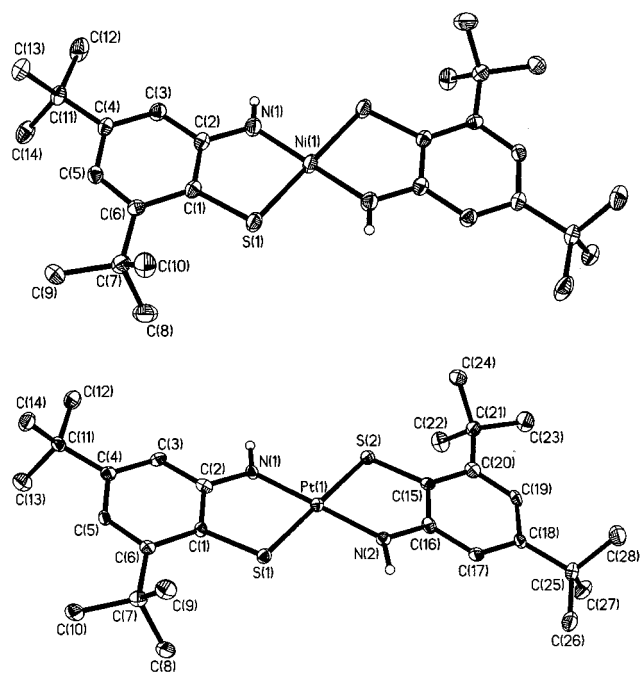(13) *ShelXTL*, Vers. 5; Siemens Industrial Automation, Inc.: 1994.

Figure 1. Structures of the neutral molecules in crystals of [**1a**]·dmf (top) and [**3a**]·CH₂Cl₂ (bottom). The small open circles represent imino hydrogen atoms.

molecules in **1a** and **3a**; Figure 2 that of **2**. Selected bond distances are summarized in Table 2.

The structures of **1a** and **3a** establish that the neutral molecules [M(L^{ISQ})₂]⁰ are square-planar and adopt a *trans*-configuration of the two ligands in the solid state. The oxygen atom of the solvent molecule dimethylformamide in **1a** is involved in hydrogen bonding contact N−H···O to the imine protons of the (L^{ISQ})$^{1-}$ ligands (O(20)···N(1) 3.078 Å), whereas the Ni-coordinated sulfur atom is not involved in any hydrogen bonding. In contrast, in **3a** neighboring molecules form inter-molecularly four weak N−H···S contacts (N(1)···S(1′) 3.373 Å, N(2)···S(2″) 3.438 Å).

The geometrical details of the *N,S*-coordinated (L^{ISQ})$^{1-}$ ligands in **1a** and **3a** show that the oxidation level is above that of *N,S*-coordinated *o*-aminothiophenolates: (i) The C−S and C−N bond lengths display considerable double bond character and (ii) the six-membered rings exhibit distortions typical of quinoid type structures, namely two shorter C=C and four longer ones. The C−S bond lengths in **3a** at ∼1.74 Å are slightly longer than those at 1.724 Å in **1a** due to the N−H···S contacts. As we will show below these features are characteristic for *N,S*-coordinated *o*-iminothionebenzosemiquinonates(1-). In the crystal structure of [Pt(S(NH)C₆H₄)₂] the C−S bonds are also very short at 1.713(7) Å as are the C−N bonds at 1.344(8) Å indicating an unperturbed *o*-iminothionesemiquinonato oxidation level.[10] The phenyl rings also clearly show the quinoid-type distortions.

As shown in Figure 2 the structure of **2** [NHEt₃][CH₃CO₂] consists of neutral *cis*-[Pd(L^{AP})₂] molecules, triethylammonium cations and acetate anions. Each acetate anion forms three N−H···O hydrogen bonding contacts. Both *cis*-coordinated NH₂ groups of *cis*-[Pd(L^{AP})₂] bind weakly to two oxygen atoms of one CH₃CO₂⁻ (N(1)···O(40) 2.871 Å, N(2)···O(41) 2.899 Å); in addition, one of these oxygens is strongly bound via another N−H···O contact (N(50)···O(40) 2.664 Å) to a triethylammonium cation. Thus, crystals of **2** comprise supramolecular {[Pd-(L^{AP})₂][NHEt₃][CH₃CO₂]}₂ entities which persist in CH₂Cl₂ solution (as shown by ¹H NMR spectroscopy), but not in donor
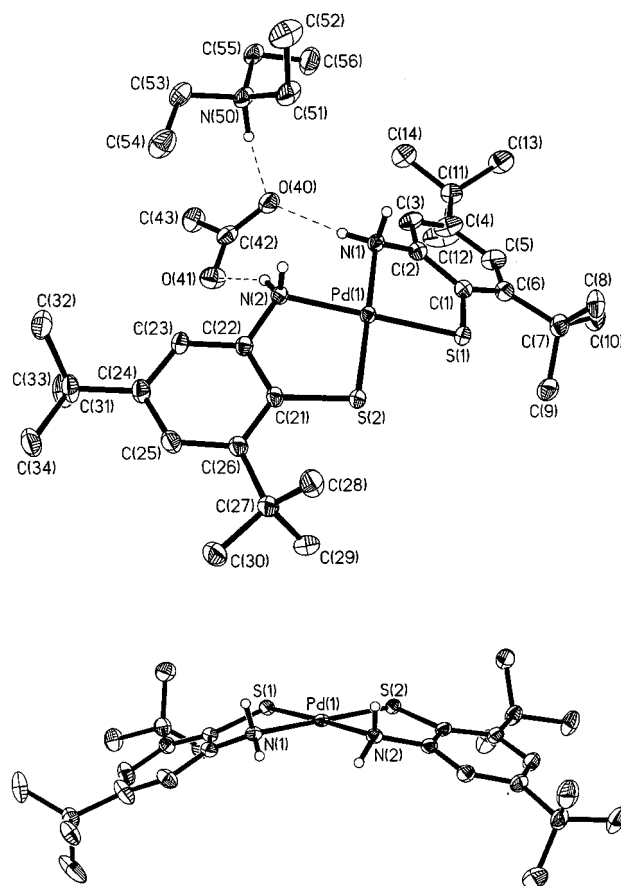

Figure 2. Structure of the isolated [Pd(L^{AP})₂][HNEt₃][CH₃CO₂] entity in crystals of [**2**][HNEt₃][CH₃CO₂] (top) and a side-view of the [Pd-(L^{AP})₂] moiety. Small open circles represent hydrogen atoms of the coordinated amino groups. Figure S1 gives a schematic view of the dinuclear entity {[Pd(L^{AP})₂][HNEt₃][CH₃CO₂]}₂.

Table 2. Selected Bond Distances (Å)

	[**1a**]·dmf	**2**[NHEt₃][CH₃CO₂]^a	**3a**·CH₂Cl₂^a
M−N	1.792(3)	2.061(1), 2.061(1)	1.928(4), 1.929(4)
M−S	2.151(1)	2.2818(4), 2.2759(6)	2.264(2), 2.273(2)
C1−S	1.724(3)	1.789(2), 1.787(2)	1.738(5), 1.743(5)
C2−N	1.348(4)	1.450(2), 1.455(2)	1.345(7), 1.341(7)
C1−C2	1.418(4)	1.397(2), 1.398(2)	1.424(7), 1.420(8)
C2−C3	1.411(4)	1.387(2), 1.385(2)	1.414(7), 1.413(7)
C3−C4	1.364(4)	1.388(3), 1.391(2)	1.366(8), 1.366(8)
C4−C5	1.424(4)	1.392(3), 1.401(3)	1.409(7), 1.423(8)
C5−C6	1.384(4)	1.404(3), 1.404(2)	1.374(6), 1.373(7)
C1−C6	1.431(4)	1.422(2), 1.419(2)	1.413(7), 1.418(8)

^{a} The first column gives the distances of the first ligand, the second those of the second.

solvents such as CH₃CN or alcohols or acetone. Figure S1 displays this dinuclear entity. Although the PdN₂S₂ coordination polyhedron is square-planar, the two phenyl rings are slightly tilted toward each other out of this plane due to the fact that the amine groups contain sp³-hybridized nitrogen atoms. Interestingly, the geometrical parameters of the *N,S*-coordinated (L^{AP})$^{1-}$ ligands clearly display the *o*-aminothiophenolates(1-) oxidation level: (i) the C−S and C−N bonds are long and typical for single bonds; (ii) five of the six C−C bonds of the phenyl rings are equidistant at an average 1.395 ± 0.006 Å;
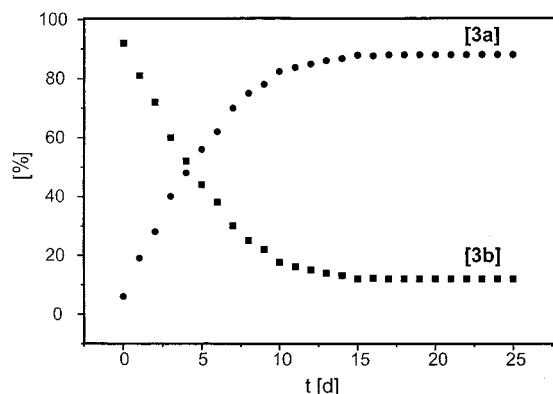
Figure 3. ^{1}H NMR spectroscopic determination of the ratio [**3a**]:[**3b**] in CH$_2$Cl$_2$ solution at 300 K as a function of time using a solution of **3a** at $t = 0$; the same plot is observed using a solution of **3b**.

only the C1−C6 distance at 1.421(2) Å is slightly−but significantly−longer. This is most probably due to the fact that C1 is bound to a sulfur atom and the neighboring C6 to a tertiary butyl group. Thus, coordinated (L^{AP})$^{1-}$ does not display the quinoid type distortions of (L^{ISQ})$^{1-}$ observed in **1a** and **3a**.

cis/trans-Equilibrium and Kinetic Studies. When a solid sample of the *cis/trans*-mixture of **3a**, **3b** as obtained from the reaction mixture described in the Experimental Section was dissolved in CH$_2$Cl$_2$ at 20 °C, its immediately recorded ^{1}H NMR spectrum (300 K) displays two sets of signals corresponding to signals of **3a** and **3b** in a ratio 70:30. At 300 K the ratio changes very slowly within days until equilibrium is reached. Thus the *cis* ⇌ *trans* isomerization reaction is very slow at 300 K. Chromatographically pure samples of **3a** and **3b** dissolved in CH$_2$Cl$_2$ at 20 °C display each a single set of signals at 300 K which were unambiguously assigned since the crystal structure of *trans*-[Pt(L^{ISQ})$_2$] **3a** has been determined by X-ray crystallography.

We have studied the kinetics of the *trans* ⇌ *cis* equilibration kinetics, eq 1, at 300 K.

$$trans\text{-}[M^{II}(L^{ISQ})_2] \underset{k_{-1}}{\overset{k_1}{\rightleftharpoons}} cis\text{-}[M^{II}(L^{ISQ})_2] \qquad (1)$$
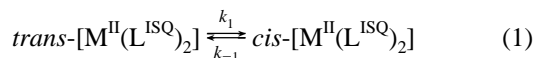
$$[cis\text{-}[ML_2]]/[trans\text{-}[ML_2]] = K = k_1/k_{-1}; \; k_{eq} = (k_1 + k_{-1}) \qquad (2)$$

Figure 3 shows the time-dependence of the intensity of the tertiary butyl ^{1}H NMR signals defined as ratio [*cis*]/[*trans*] of a CH$_2$Cl$_2$ solution of **3a**. Exactly the same curves are observed when **3b** is the starting material. Both curves can be fitted by using a simple exponential function (first-order process) yielding a first-order rate constant, $k_{eq} = 2.3 \times 10^{-6}$ s^{-1}. The equilibrium constant, K, is 0.14 at 300 K. From this information the rate constants k_1, k_{-1} are established to be 2.7×10^{-7} s^{-1} and 2.0×10^{-6} s^{-1}, respectively; and $\Delta G° = -RT \ln K$ yields 5.0 ± 0.5 kJ mol^{-1} at 300 K.

In contrast, the ^{1}H NMR spectrum recorded at 300 K of the deep blue material **1a/1b** obtained from the reaction mixture and dissolved in CH$_2$Cl$_2$ at 300 K displays only two sharp proton signals for two chemically inequivalent tertiary butyl groups at $\delta = 1.29$ and 1.75 ppm. On lowering the temperature these signals broaden and then split into two sets of signals which we assign to the *trans*- and *cis*-isomer, respectively. This assignment is based on the observation that in the *trans*-isomer **3a** the difference between the two *tert*-butyl signals is larger (0.40 ppm) than for the *cis*-isomer **3b** (0.35 ppm). A dynamic equilibrium where the rate of equilibration is of the order of an
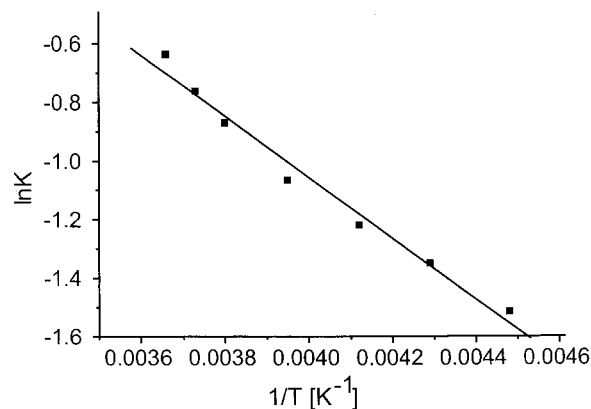
^{1}H NMR experiment ($\sim 10^{-5}$ s) is observed. Thus equilibration of **1a/1b** is much faster than that of **3a/3b**.

We have determined the temperature-dependence of the *trans*/*cis*-ratio **1a/1b** which is shown in form of a Van't Hoff plot in Figure 4. From this the following thermodynamic parameters were established: $\Delta G° = 1.9 \pm 0.2$ kJ mol^{-1}; $\Delta H° = 1.6 \pm 0.1$ kJ mol^{-1}; $\Delta S° = -0.9 \pm 0.4$ J mol^{-1} K^{-1}. Thus at 20 °C the *trans*-isomer **1a** is thermodynamically the favored form in CH$_2$Cl$_2$ solution (**1a:1b** ≈ 70:30).

Finally, a CH$_2$Cl$_2$ solution of **2a/2b** (as isolated) at 298 K contains a 75:25 mixture of **2a:2b**. The rate of equilibration is of the order of minutes and thus faster than its Pt-analogue but slower than its Ni-analogue. The rate of equilibration is too fast for a separation of isomers using HPLC methods.

All electrochemical experiments and spectroscopic measurements in CH$_2$Cl$_2$ solutions of **1a/1b** and **2a/2b** pertain to the equilibrium mixture of the *trans*- and *cis*-isomers at a given temperature (20 °C). Only **3a** and **3b** were separated; both species are kinetically rather stable in solution at 20 °C.

Electro- and Spectroelectrochemistry. The electrochemistry of complexes **1a/1b**, and **2a/2b** mixtures (see above) and of pure **3a** and **3b** has been studied in CH$_2$Cl$_2$ solutions containing 0.10 M [(*n*-Bu)$_4$N]PF$_6$ as supporting electrolyte by cyclic voltammetry. Ferrocene was used as an internal standard, and all redox potentials are referenced versus the ferrocenium/ferrocene (Fc$^+$/Fc) couple. The results are summarized in Table 3.

All neutral complexes display similar electrochemical behavior; they all undergo two successive, reversible one-electron reductions and two successive, one-electron oxidations.[7−9] Figure 5 (bottom) shows a typical cyclic voltammogram (CV) for **3a**. This corresponds to the expected complete electron-transfer series known for many square-planar complexes of this type. Thus, the di-, and monocations and di-, and monoanions as well as the neutral species are accessible. Matsumoto et al.[10] have reported similar results for *trans*-[Pt(S(NH)C$_6$H$_4$)$_2$] containing the unsubstituted derivative of (L^{AP})$^{1-}$ and (L^{ISQ})$^{1-}$. The effect of the four tertiary butyl groups in our complexes is clearly reflected in the observed redox potentials. Our ligand is more electron-rich than the corresponding unsubstituted ligand, and consequently, the neutral square-planar complexes, [M(L^{ISQ})$_2$], are easier to oxidize by 250−300 mV but more difficult to reduce by ∼300 mV than their unsubstituted analogues.

Significantly, the redox potentials $E^1_{1/2}$, $E^2_{1/2}$, $E^3_{1/2}$, and $E^4_{1/2}$ measured for **3a** and **3b** do not differ much (15−50 mV), indicating that the structural difference is not an important factor. From this and the ^{1}H NMR measurements (see above) we

Figure 4. Van't Hoff plot of the temperature dependence of the *cis* ⇌ *trans* equilibrium constant of **1a/1b**.

Table 3. Summary of Redox Potentials of Complexes[a]

	$E^1_{1/2}(2\text{-}/1\text{-})$, V	$E^2_{1/2}(1\text{-}/0)$, V	$E^3_{1/2}(0/1+)$, V	$E^4_{1/2}(1+/2+)$, V
1a/1b	−1.714	−0.826	0.284	0.896(irr.)
2a/2b	−1.484	−0.790	0.264	0.833
3a	−1.535	−0.698	0.513	1.195
3b	−1.519	−0.732	0.456	1.183
[Pt^{II}(S-(NH)C$_6$H$_4$)$_2$][b]	−1.202(q.r.)	−0.421(q.r.)	0.753(q.r.)	not observed

[a] Conditions: CH$_2$Cl$_2$ solution 0.10 M [(*n*-Bu)$_4$N]PF$_6$; glassy carbon working electrode; ferrocene internal standard; 22 °C; scan rate 100 mV s^{-1}; potentials are referenced versus the ferrocenium/ferrocene (Fc$^+$/Fc) couple. [b] Acetone solution 0.05 M [(*n*-Bu)$_4$N]ClO$_4$; ref 10. irr. = irreversible, q.r. = quasi-reversible.
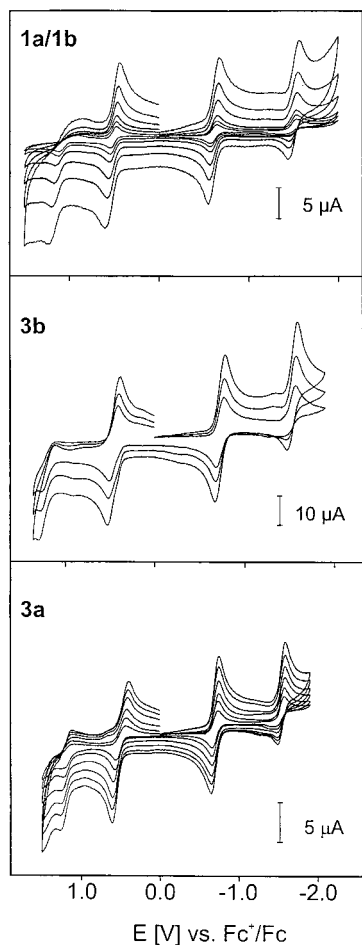
Figure 5. Cyclic voltammograms of a mixture of *trans*/*cis*-[Ni(L^{ISQ})$_2$] (**1a**/**1b**) (∼70:30), of *cis*-[Pt(L^{ISQ})$_2$] (**3b**) and of *trans*-[Pt(L^{ISQ})$_2$] (**3a**). Scan rates: **1a**/**1b**: 50, 100, 200, 500, 1000, 2000 mV s^{-1}; **3b**: 200, 400, 800 mV s^{-1}; **3a**: 50, 100, 200, 300, 400, 500 mV s^{-1}. Conditions: 22 °C; CH$_2$Cl$_2$ solutions containing 0.10 M [(*n*-Bu)$_4$N]-PF$_6$; glassy carbon working electrode.

conclude that the electrochemical data (Table 3) for **1a**/**1b** and **2a**/**2b** mixtures are predominantly those of **1a** and **2a**, respectively, since the *trans*-isomers are the dominating species (∼70%) in CH$_2$Cl$_2$ solution and contributions from the *cis*-isomers cannot be resolved by cyclic voltammetry (or square-wave voltammetry).

The electronic spectra of electrochemically generated oxidized and reduced forms of **3a** and of **1a**/**1b** have been recorded and are shown in Figures 6 and 7, respectively; Table 4 summarizes the spectral results.

The electronic spectra of the neutral complexes **1a**/**1b**, **2a**/**2b**, and of **3a** and **3b** are dominated by an intense ligand-to-ligand charge-transfer band (LLCT) in the near-infrared in the range 730−840 nm. This LLCT band is a spin- and dipole-allowed transition which is observed in all square-planar
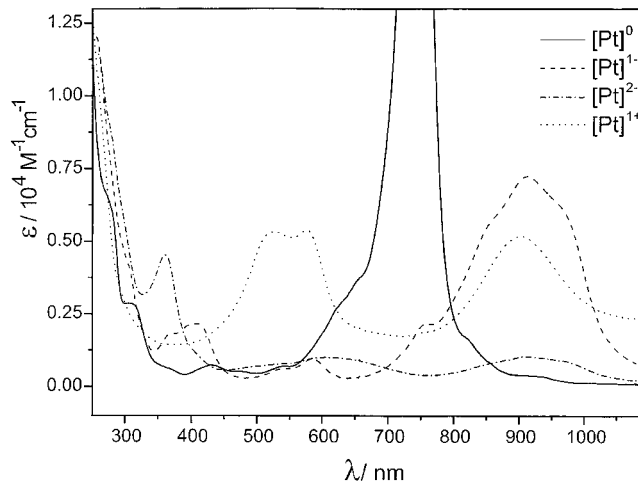

Figure 6. Electronic spectra of the electrochemically oxidized and reduced forms of [**1a**/**1b**] in CH$_2$Cl$_2$ solution (0.10 M [(*n*-Bu)$_4$N]PF$_6$) at −40 °C. The spectrum of the neutral species is also included.
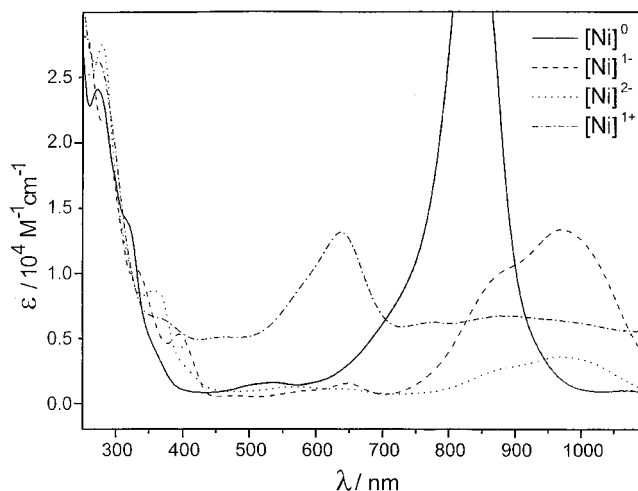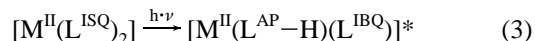

Figure 7. Electronic spectra of the electrochemically oxidized and reduced forms of **3a** in CH$_2$Cl$_2$ solution (0.10 M [(*n*-Bu)$_4$N]PF$_6$) at −40 °C. The spectrum of the neutral species is also included.

complexes of Ni^{II}, Pd^{II}, Pt^{II} containing two bidentate benzosemi-quinonato-type ligands, eq 3.[3]

$$[M^{II}(L^{ISQ})_2] \xrightarrow{h\cdot\nu} [M^{II}(L^{AP}-H)(L^{IBQ})]^* \qquad (3)$$

$$(S=0), \quad \mu = 0 \qquad (S=0), \quad \mu \neq 0$$

Upon ligand-centered one-electron oxidation or reduction of these neutral species this transition is, in general, quenched. It is noteworthy that the LLCT transition is observed in the spectrum of the *trans*-isomer **3a** at 732 nm ($\epsilon = 9.1 \times 10^4$ L mol^{-1}cm^{-1}) but at 751 nm (9.1×10^4) for its *cis*-isomer **3b**.

Compounds containing two *o*-aminothiophenolate(1-) ligands, (L^{AP})$^{1-}$, such as **1** and **2** do not exhibit transitions >350 nm
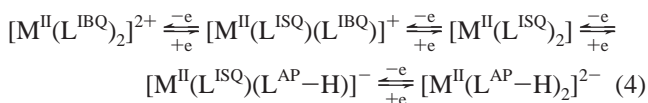
Table 4. Electronic Spectra of Complexes in CH_2Cl_2 Solution[a]

complex	λ_{max}, nm ($10^4 \epsilon$, L mol^{-1} cm^{-1})
1	280sh, 305(2.9)
1a/1b	280(2.4), 320sh, 508(0.02), 837(8.7)
*[**1a/1b**]$^-$	258(2.6), 275(2.7), 359sh, 393(0.5), 650(0.1), 840sh(0.9), 971(1.3)
*[**1a/1b**]$^+$	274(1.7), 326(0.8), 640(1.3), 800−1000(0.6)
2	278(2.7), 298(3.0)
2a/2b	245(10), 328sh, 544(0.25), 822(7.4)
3a	241(6.0), 283sh, 310(1.2), 433(0.21), 623sh, 732(9.1)
3b	242(5.0), 283sh, 310(0.8), 433(0.19), 623sh, 751(9.1)
*[**3a**]$^-$	231(3.3), 256(3.2), 305sh, 362sh, 411(0.2), 542sh, 585(0.1),766sh, 853sh, 916(0.8), 980sh
*[**3a**]$^+$	236(1.21), 528(0.5), 577(0.5), 904(0.5)

[a] The asterisks denote species generated electrochemically at −40 °C in CH_2Cl_2 solutions containing 0.10 M [(*n*-Bu)$_4$N]PF$_6$.

with extinction coefficients >400 L mol^{-1} cm^{-1}. Similarly, compounds containing two *o*-iminothiophenolates(2-) ligands, (L^{AP}−H)$^{2-}$, such as the dianionic species [M^{II}(L^{AP}−H)$_2$]$^{2-}$ (M = Ni, Pt) do not exhibit absorptions >400 nm of intensity >500 L mol^{-1} cm^{-1}. The absorptions at >400 nm seen in the spectra of the [M(L^{AP}−H)$_2$]$^{2-}$ species in Figures 6 and 7 are due to incomplete electrolytic reductions of the monoanionic precursors (∼10% of these species are still present). We can safely assign the following oxidation levels for the ligands and metal ions in the dianions as [M^{II}(L^{AP}−H)$_2$]$^{2-}$ (M = Ni, Pt).

The spectra of the monocations of **1a/1b** and **3a** are similar; both exhibit an intense intraligand $\pi-\pi^*$ CT band at 640 and 560 nm which we assign to a coordinated *o*-iminothionequinone ligand, (L^{IBQ}). These absorption maxima also appear for the rapidly generated dications [M^{II}(L^{IBQ})$_2$]$^{2+}$, but they are not stable enough, even at low temperatures, to allow their full characterization. In addition, a very broad absorption at ∼900 nm is observed in both monocations with $\epsilon \approx 5000$ L mol^{-1} cm^{-1} which is tentatively assigned to an *o*-iminothionesemiquinonate ligand radical, (L^{ISQ})$^{1-}$. Thus, an electronic structure of [M^{II}-(L^{IBQ})(L^{ISQ})]$^+$ (M = Ni, Pt) with an $S = ^1/_2$ ground state is proposed for both monocations. This implies that the unpaired electron is predominantly localized on the ligand. A description of their electronic structure as [M^{III}(L^{ISQ})$_2$]$^+$ implying a metal-centered oxidation of **1a/1b** and **3a** can be ruled out since the expected intraligand LLCT band is not observed (see also below).

The spectra of the monoanions of **1a/1b** and **3a** are also quite similar and interesting since both species exhibit an intense absorption at 971 and 916 nm with $\epsilon \approx 10^4$ L mol^{-1} cm^{-1} but no or weak absorptions at 640 nm. This indicates to us that these species contain at least one (L^{ISQ})$^{1-}$ ligand as in [M^{II}-(L^{ISQ})(L^{AP}−H)]$^-$. It is interesting that the spectra of the mono- and dianions, and mono- and dications of bis(aminophenolate)-metal complexes of Pd^{II} are very similar to those reported here.[3b] These spectral and electrochemical results lead us to the conclusion that the redox activity of the present series of [M^{II}-(L^{ISQ})$_2$] complexes is predominantly ligand-based as shown in eq 4.

$$[M^{II}(L^{IBQ})_2]^{2+} \underset{+e}{\overset{-e}{\rightleftharpoons}} [M^{II}(L^{ISQ})(L^{IBQ})]^+ \underset{+e}{\overset{-e}{\rightleftharpoons}} [M^{II}(L^{ISQ})_2] \underset{+e}{\overset{-e}{\rightleftharpoons}}$$

$$[M^{II}(L^{ISQ})(L^{AP}-H)]^- \underset{+e}{\overset{-e}{\rightleftharpoons}} [M^{II}(L^{AP}-H)_2]^{2-} \quad (4)$$

Both the monocations and the monoanions of **1a/1b** and **3a** are paramagnetic species with an $S_t = ^1/_2$ ground state. We have recorded their X-band EPR spectra which are shown in Figures 8 and 9, respectively; *g*-values and hyperfine coupling constants obtained from simulations are given in Table 5. These spectra closely resemble those reported for many analogous mono-anionic and monocationic species containing M^{II}−O$_4$, M^{II}−N$_4$,
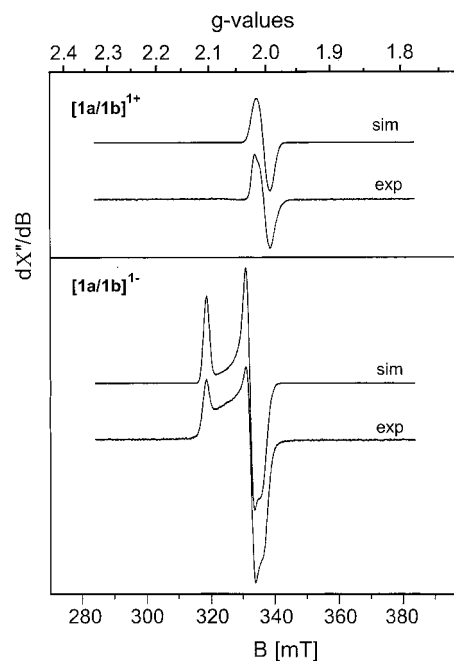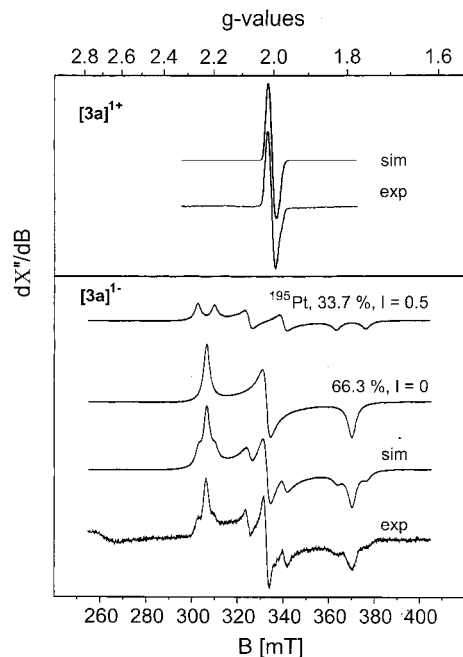

Figure 8. X-band EPR spectra of the monocation (top) and monoanion (bottom) of [Ni(L^{ISQ})$_2$] (**1a/1b**) in frozen CH_2Cl_2 solution (0.10 M [(*n*-Bu)$_4$N]PF$_6$) at 10 K.

M^{II}−N$_2$O$_2$, and M−N$_2$S$_2$ cores (M = Ni, Pt) and we refer to their careful discussion in ref 7 and 8. The most interesting case here is that of the reduced and oxidized forms of **3a** where ^{195}Pt hyperfine coupling is observed for both species. The spectrum of [**3a**]$^-$ displays $g_z > g_{x,y}$ and a large hfc constant $A_{iso}(^{195}$Pt) of 109 G, whereas for [**3a**]$^+$ this hfc constant is only 9.5 G. The spectrum of [**3a**]$^-$ indicates to us that the unpaired electron possesses considerable metal d orbital, ($d_{x^2-y^2}$), character lending support to the notion that the central Pt ions has some Pt(I) character with ($d_{x^2-y^2}$)^1 electron configuration. In contrast, the spectra of the monocations support the idea of a predominantly ligand-centered organic radical since the g_{iso} values of 2.0014 and 2.0073 are close to those observed for uncoordinated organic free radicals. No evidence for metal-centered oxidations has been detected.

Simulation of Magnetically Perturbed Mössbauer Spectra of [Fe^{II}(L$^{\bullet\bullet}$)(PR$_3$)]. Recently Sellmann et al.[6] reported the synthesis, crystal structures, and spectroscopic characterization of two five-coordinate iron complexes containing two *N,S*-coordinated *o*-amidothiophenolate entities and a triphenylphosphane, or tris(*n*-propyl)phosphane ligand. The structure of the triphenylphosphane complex is reproduced in Figure 10. These authors have considered the ligand as redox innocent tetraanion 1,2-ethanediamido-*N,N′*-bis(2-benzenethiolato)(4-) and described its electronic structure as iron(IV) (*S* = 1) species in agreement

**Table 5.** EPR Spectroscopic Data of Complexes in CH_2Cl_2 Solution (0.10 M [(n-Bu)$_4$N]PF$_6$)

complex	g_x	g_y	g_z	g_{iso}	A_{xx}, G	A_{yy}, G	A_{zz}, G
[**1a/1b**]$^-$	2.0282	2.0055	2.1147	2.067			
[Ni(S(NH)C$_6$H$_4$)$_2$]$^{- a}$	2.028	2.005	2.126	2.053			
[**1a/1b**]$^+$	1.9970	1.9901	2.0172	2.0014			
[**3a**]$^-$	1.8270	2.0313	2.2054	2.021	75	142	110
[**3a**]$^+$	1.9976	2.0151	2.0092	2.0073	10.4	9.7	8.3

^{a} References 7, 8.

Figure 9. X-band EPR spectra of the monocation (top) at 10 K and monoanion (bottom) at 60 K of *trans*-[Pt(L^{ISQ})$_2$] (**3a**) in frozen CH$_2$-Cl$_2$ solution (0.10 M [(n-Bu)$_4$N]PF$_6$].
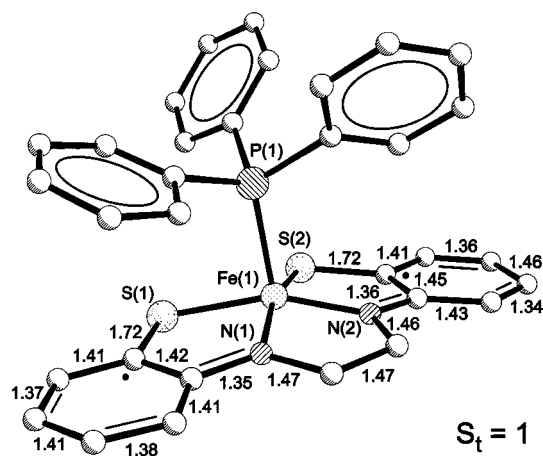
Figure 10. Structure of [Fe^{II}(L$^{\bullet\bullet}$)(PPh$_3$)] from ref 6. Bond distances are from the Cambridge Crystallographic Data Centre No. CSD-406038.

with a room-temperature magnetic moment of 2.76 μ_B (295 K). They also reported zero- and applied field (2.5 and 5.0 T) Mössbauer spectra at 4.2 K ($\delta = 0.04$ mm s^{-1}, $|\Delta E_Q| = 3.16$ mm s^{-1}) but did not perform a spin-Hamiltonian analysis.

Inspection of the geometrical details of the alleged *o*-amidothiophenolato(2-) entities in the structure reveals all the typical characteristics of *o*-iminothionesemiquinonate(1-) ligands which implies a *physical*[14] oxidation state of +II for the iron center.

(14) Jörgensen, C. K. In *Oxidation Numbers and Oxidation States*; Springer: Heidelberg, Germany, 1969.
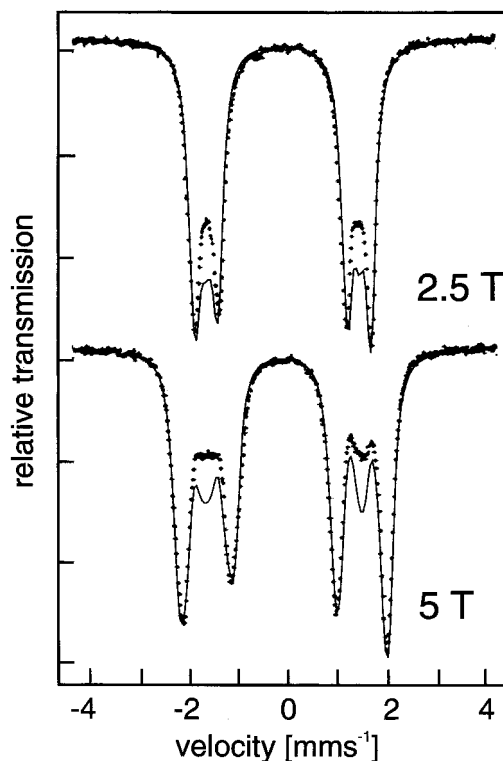
Figure 11. Applied-field Mössbauer spectrum at 4.2 K and simulations (solid lines) of [Fe^{II}(L$^{\bullet\bullet}$){P(i-propyl)$_3$}]. The data were taken from ref 6. For simulation parameters see text.

The observed $S_t = 1$ ground state is then achieved via a strong intramolecular, ferromagnetic coupling of the two organic radicals mediated by a low-spin ferrous ion. The two possibilities for the electronic structure I and II should be
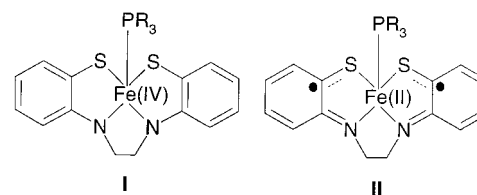
readily discerned by a spin-Hamiltonian analysis of the applied-field Mössbauer spectra.

The experimental magnetic Mössbauer spectra measured at 4.2 K and applied fields (field orientation not reported, but assumed here to be $B_{||} \gamma$-beam) from the original paper[6] together with spin-Hamiltonian simulations for $S_t = 1$ from our group are shown in Figure 11.

The magnetic hyperfine splittings of the spectra reveal the presence of a *very weak* induced internal field of only ~1 T at 5 T applied field. Such weak fields can originate from either an Fe(IV) ($S_{Fe} = 1$) valence state and *very large zero-field splitting* (ZFS) or from a low-spin ferrous ion ($S_{Fe} = 0$) and a ligand diradical, L$^{\bullet\bullet}$, with a spin triplet ground state $S_t = 1$. In

10020 *J. Am. Chem. Soc., Vol. 123, No. 41, 2001*

Herebian et al.

the former case the internal field at the ^{57}Fe nucleus originates from an Fe(IV) "$m_s = 0$" magnetic ground state which has induced magnetization due to level mixing by the applied field. The magnitude of this effect depends then on the applied field strength and the energy of the ZFS. For genuine Fe(IV) ($S_{Fe} = 1$) the ZFS can be as large as $\sim$20 cm^{-1} which dominates the Zeeman interaction ($D \gg \mathbf{g} \cdot \mu_B \mathbf{B}$). In the latter diradical case the Mössbauer nucleus experiences a *transferred hyperfine field* due to covalent delocalization of radical spin density into the iron valence orbitals. The ZFS of a spin triplet state of a diradical is small and usually of the order of $\sim$0.1 cm^{-1}, because only the spin dipolar coupling generates an effective ZFS of the triplet.

In both above regimes of ZFS it has been possible to obtain reasonable simulations of the magnetically perturbed spectra of [Fe(L$^{••}$)(PR$_3$)]. However, the observed very low strength of the internal field requires an unreasonably large value for D and, also, unreasonably low values for the components of the hyperfine coupling tensor $\mathbf{A}$ for the model involving an Fe(IV) ($S_{Fe} = 1$). Thus, a fit to the published data yields $D \approx 100$ cm^{-1} (!) and $A_i/g_N\beta_N \approx -8$ T. For genuine Fe(IV) ($S_{Fe} = 1$) complexes with a(d$_{xy}$)^2(d$_{xz}$, d$_{yz}$)^2 configuration D would be $\sim$20 cm^{-1} and $A_i/g_N\beta_N = -16$ T.
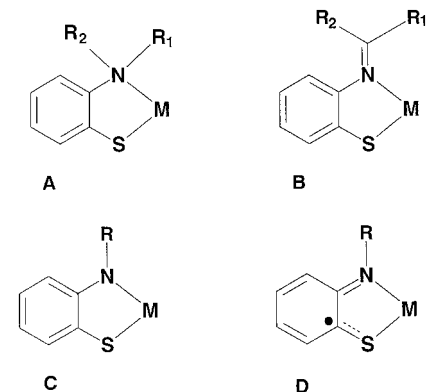
On the other hand, a better and physically more reasonable fit was obtained for a model involving a low-spin Fe(II) ion ($S_{Fe} = 0$) and a triplet diradical ($S_t = 1$) with small ZFS. Since the magnetic Mössbauer spectra are not very sensitive to the actual value of the ZFS in this regime, we fixed D at 0.1 cm^{-1} and $E/D = 0$. Optimization of the $\mathbf{A}$ tensor components yields $A_i/g_N\beta_N = (-1, -1, -1.2)$ T. These values are fully consistent with spin density delocalization and are only 5–10% of what is expected for an iron-centered spin system. Thus, the fit in Figure 11 has been obtained using the following parameters: $\delta = 0.04$ mm s^{-1}, $\Delta E_Q = -3.16$ mm s^{-1}, $\eta = 0.7$, D = 0.1 cm^{-1}, $E/D = 0$, and $A_i/g_N\beta_N = (-1, -1, -1.2)$ T. It is important to note that the *negative* sign of the electric quadrupole splitting obtained for both models is not consistent with the (d$_{xy}$)^2(d$_{xz}$, d$_{yz}$)^2 configuration of an Fe(IV) ($S_{Fe} = 1$).

The complexes [Fe^{II}(L$^{••}$)(PR$_3$)] are interesting and important in the context of our proposed noninnocence of *o*-aminothiophenolates since they unambiguously display the presence of two *N,S*-coordinated *o*-iminothionebenzosemiquinonate(1-) radicals.

Discussion

Evaluation of Published Structures. A search of the Cambridge Crystallographic Data Centre produced about 120 structures of transition metal complexes containing at least one *N,S*-coordinated *o*-aminothiophenolato derived moiety. At this point, the formal charge or the oxidation level of this moiety was not specified. A careful inspection of these data revealed that it is possible to identify four distinctly different categories of compounds as shown schematically in Table 6: (1) the majority of compounds contains a monoanionic *N,S*-coordinated *o*-aminothiophenolato(1-) entity where the amino nitrogen is four coordinate (sp^3 hybridized) as in the motif A; (2) a number of compounds contain a ligand derivative where the amino nitrogen forms an N=C double bond (Schiff base) yielding an sp^2 hybridized nitrogen donor as in motif B; (3) the *o*-aminothiophenolate ligand in A can be deprotonated yielding a dianionic *N,S*-coordinated *o*-imidothiophenolato(2-) ligand as in motif C and, finally, (4) this dianion can be one-electron oxidized yielding an *N,S*-coordinated radical anion, namely the *o*-iminothionesemiquinonate(1-). We have not found a single structure where a neutral *N,S*-coordinated *o*-iminothionequinone has been unequivocally identified.

Table 6. Categories of Complexes Containing an *N,S*-coordinated *o*-Aminothio- Phenolato Derivative and Average C−S and C−N Bond Lengths

type	av C−S, Å^a	av C−N, Å^a	nature of phenyl ring	n^b
A	1.756	1.464	aromatic	39
B^c	1.756	1.435	aromatic	24
C	1.755	1.413	aromatic	11
D	1.724	1.356	quinoid	25

^{a} Estimated error $\pm$0.03 Å (3σ). ^{b} Number of crystallographically independent *o*-aminothiophenolate entities used in the analysis. ^{c} The average N=C bond distance of the Schiff base is 1.29 $\pm$ 0.02 Å.

For the following discussion of the geometrical differences between these categories, we have selected those structures where the physical oxidation state of the central metal ion has been unambiguously established by spectroscopic or other structural considerations. This allows us, in general, to determine the oxidation level of the ligand and discern between complexes belonging to categories C and D, respectively. Those belonging to A and B are, of course, readily identified by their respective geometries at the nitrogen donor atom.

Table 6 summarizes the results of the analysis. In all complexes of category A[15−31] the S−C$_{phenyl}$ bond length is found at 1.756 $\pm$ 0.02 Å corresponding to a typical thiophenolato C−S single bond and—at the same time—the N−C$_{phenyl}$ bond distance

(15) Takác, J.; Soós, E.; Nagy-Magos, Z.; Markó, L.; Gervasio, G.; Hoffmann, T. *Inorg. Chim. Acta* **1989**, *166*, 39.

(16) Vicente, J.; Chicote, M. T.; Bermúdez, M. D.; Jones, P. G.; Fittschen, C.; Sheldrick, G. M. *J. Chem. Soc., Dalton Trans.* **1986**, 2361.

(17) Brand, U.; Vahrenkamp, H. *Z. Anorg. Allg. Chem.* **1996**, *622*, 213.

(18) Sellmann, D.; Ruf, R.; Knoch, F.; Moll, M. *Z. Naturforsch.* **1995**, *50b*, 791.

(19) Ueyama, N.; Tuji, T.-A.; Okamura, T.-A.; Nakamura, A. *Acta Crystallogr.* **1998**, *C54*, 1424.

(20) Janssen, M. D.; Grove, D. M.; van Koten, G.; Spek, A. L. *Recl. Trav. Chim. Pays-Bas* **1996**, *115*, 286.

(21) Brand, U.; Vahrenkamp, H. *Chem. Ber.* **1996**, *129*, 435.

(22) Küsthardt, U.; Albach, R. W.; Kiprof, P. *Inorg. Chem.* **1993**, *32*, 1838.

(23) Dickman, M. H.; Doedens, R. J.; Deutsch, E. *Inorg. Chem.* **1980**, *19*, 945.

(24) Dowerah, D.; Spence, J. T.; Singh, R.; Wedd, A. G.; Wilson, G. L.; Farchione, F.; Enemark, J. H.; Kristofzski, J.; Bruck, M. *J. Am. Chem. Soc.* **1987**, *109*, 5655.

(25) Sellmann, D.; Emig, S.; Heinemann, F. W.; Knoch, F. *Z. Naturforsch.* **1998**, *53b*, 1461.

(26) Sellmann, D.; Reineke, U.; Huttner, G.; Zsolnai, L. *J. Organomet. Chem.* **1986**, *310*, 83.

(27) Barnard, K. R.; Bruck, M.; Huber, S.; Grittini, C.; Enemark, J. H.; Gable, R. W.; Wedd, A. G. *Inorg. Chem.* **1997**, *36*, 637.

(28) Tsagkalidis, W.; Rodewald, D.; Rehder, D. *Inorg. Chem.* **1995**, *34*, 1943.

(29) Piggott, B.; Woug, S. F.; Williams, D. J. *Inorg. Chim. Acta* **1988**, *141*, 275.

(30) Hahn, R.; Nakamura, A.; Tanaka, K.; Nakayama, Y. *Inorg. Chem.* **1995**, *34*, 6562.

(31) Sellmann, D.; Utz, J.; Heinemann, F. W. *Inorg. Chem.* **1999**, *38*, 459.

is found at 1.46 ± 0.02 Å as in aniline. The phenyl ring is aromatic with six equivalent C−C bond lengths. Due to thermal motion and crystallographic problems of structure determinations at room temperature, the range of observed C−C lengths in a given structure can be rather large ($1.43-1.32$ Å) but it is significant that in no instance systematic deviations pointing to a quinoid type structure have been detected.

Similarly, in complexes of type B^{32-49} the C=N bond length of the Schiff base part is short at 1.29 ± 0.02 Å and the N−C_{phenyl} bond is found at 1.41 ± 0.02 Å which is slightly shorter than the N−C_{phenyl} bond in complexes of type A. Interestingly, the S−C_{phenyl} bond length at 1.76 ± 0.02 remains the same as in type A − it is a C−S single bond. The phenyl ring is again aromatic with, in principle, six equivalent C−C bonds.

In complexes of type C^{50-54} containing an *N,S*-coordinated dianionic *o*-amidothiophenolate(2-) the S−C_{phenyl} bond length at 1.755 ± 0.02 Å is the same as in A and B but the N−C_{phenyl} bond length at 1.41 ± 0.02 Å is significantly shorter than that in A and similar to that in B. The phenyl ring is again aromatic with six equivalent C−C bonds.

Finally, we have identified structures$^{55-70}$ where both the S−C_{phenyl} *and* the N−C_{phenyl} bond distances are significantly shorter than in all complexes of types A, B, and C. Here, in complexes of type D, the S−C_{phenyl} bond distance shrinks to 1.724 ± 0.02 Å and−*at the same time*−the N−C_{phenyl} bond length decreases to 1.356 ± 0.02 Å. Both bonds display considerable double bond character. In complexes of type D the six C−C bond distances display a pattern of one short, a long, and another short distance followed by three long C−C bonds. This is typical for coordinated *o*-semiquinonates,^{2} *o*-iminosemiquinonates,^{3} and *o*-diiminosemiquinonates.^{1} We note that this pattern is often not identifyable in room-temperature structures at the 3σ level of confidence. Therefore, previous authors dealing with a single structure at a time have often assigned these ligands into category C as *o*-amidothiophenolato(2-) species.

For example, the neutral complexes [M(abt)$_3$] (M = Mo,^{59} Tc,^{57} Re,^{63} and Os^{63}), where abt represents according to these authors the unsubstituted amidothiophenolato(2-) ligand, have been described as Mo(VI) (d^0),^{58,59} Tc(VI), Re(VI) (d^1), and Os(VI) (d^2) complexes. All species are highly colored. Their reported ligand geometries allow us to reassign the physical oxidation levels of the ligands as monoanionic π-radicals, abt$^{\bullet-}$(1-). Thus, these neutral compounds contain three *N,S*-coordinated *o*-iminothionesemiquinonato(1-) ligand π-radicals and a *trivalent* metal ion: Mo(III) d^3, Tc(III) d,^{4} Re(III) d,^{4} and Os(III) d.^{5} The observed magnetic properties and electronic ground states of these complexes are then interpreted as follows: A half-filled t$_{2g}^3$ subshell in the Mo(III) species ($S_{Mo} = {}^3/_2$) is strongly antiferromagnetically coupled to three ligand radicals ($S_{rad} = {}^1/_2$) yielding the observed $S_t = 0$ ground state as in [Cr^{III}(SQ)$_3$]^{71} and [Cr(L^{ISQ})$_3$]^{3c} where SQ represents an *O,O*-coordinated *o*-semiquinonate(1-) and L^{ISQ} is here the *O,N*-coordinated *o*-iminosemiquinonate(1-). In low-spin Tc(III) and Re(III) a t$_{2g}^4$ subshell allows the antiferromagnetic coupling of only two ligand radicals yielding an $S_t = {}^1/_2$ ground state which should be of ligand-centered origin. Consistent with this, an isotropic EPR spectrum with $g_{iso} = 2.013$ typical for organic radicals has been reported for [Re(abt)$_3$] and 2.008 for the Tc analogue.^{72} [Os(abt)$_3$] has been reported to possess an $S_t = 0$ ground state based on the observation of a "normal" ^{1}H NMR

(32) Castro, J.; Romero, J.; García-Vázquez, J. A.; Durán, M. L.; Castineiras, A.; Sousa, A.; Fenton, D. E. *J. Chem. Soc., Dalton Trans.* **1990**, 3255.

(33) Toshev, M. T.; Yusupov, V. G.; Saidov, S. O.; Karimov, Z. T.; Dustov, K. b.; Karimov, M. M.; Zelenin, K. N.; Parpiev, N. A. *Koord. Khim.* **1992**, *18*, 974.

(34) Sawusch, S.; Schilde, U. *Z. Naturforsch.* **1999**, *54b*, 881.

(35) Tahir, M. N.; Ülkü, D.; Atakol, O.; Kenar, A. *Acta Crystallogr.* **1996**, *C52*, 2178.

(36) Müller, A.; Johannes, K. U.; Plass, W.; Bögge, H.; Krahn, E.; Schneider, K. *Z. Anorg. Allg. Chem.* **1996**, *622*, 1765.

(37) Labisbal, E.; García-Vázquez, J. A.; Gómez, C.; Macias, A.; Romero, J.; Sousa, A.; Englert, U.; Fenton, D. E. *Inorg. Chim. Acta* **1993**, *203*, 67.

(38) Kawamoto, T.; Nagasawa, I.; Kuma, H.; Kushi, Y. *Inorg. Chem.* **1996**, *35*, 2427.

(39) Ülkü, D.; Tahir, M. N.; Ücar, G.; Atakol, O. *Acta Crystallogr.* **1996**, *C52*, 1884.

(40) Kawamoto, T.; Kuma, H.; Kushi, Y. *Chem. Commun.* **1996**, 2121.

(41) Brand, U.; Vahrenkamp, H. *Chem. Ber.* **1995**, *128*, 787.

(42) Bouwman, E.; Henderson, R. K.; Powell, A. K.; Reedijk, J.; Smeets, W. J. J.; Spek, A. L.; Veldman, N.; Wocadlo, S. *J. Chem. Soc., Dalton Trans.* **1998**, 3495.

(43) Craig, J. A.; Harlan, E. W.; Snyder, B. S.; Whitener, M. A.; Holm, R. H. *Inorg. Chem.* **1989**, *28*, 2082.

(44) Ercan, F.; Ülkü, D.; Ancin, N.; Oztas, S. G.; Tüzün, M. *Acta Crystallogr.* **1996**, *C52*, 1141.

(45) Farahbakhsh, M.; Nekola, H.; Schmidt, H.; Rehder, D. *Chem. Ber./Recl.* **1997**, *130*, 1129.

(46) Hahn, R.; Herrmann, W. A.; Artus, G. R. J.; Kleine, M. *Polyhedron* **1995**, *14*, 2953.

(47) Hahn, R.; Küsthardt, U.; Scherer, W. *Inorg. Chim. Acta* **1993**, *210*, 177.

(48) Goedken, V. L.; Christoph, G. G. *Inorg. Chem.* **1973**, *12*, 2316.

(49) Noveron, J. C.; Herradora, R.; Olmstead, M. M.; Mascharak, P. K. *Inorg. Chim. Acta* **1999**, *285*, 269.

(50) Cook, J.; Davis, W. M.; Davison, A.; Jones, A. G. *Inorg. Chem.* **1991**, *30*, 1773.

(51) Chi, D. Y.; Wilson, S. R.; Katzenellenbogen, J. A. *Inorg. Chem.* **1995**, *34*, 1624.

(52) Noveron, J. A.; Olmstead, M. M.; Mascharak, P. K. *J. Am. Chem. Soc.* **1999**, *121*, 3553.

(53) Rajan, O. A.; Spence, J. T.; Leman, C.; Minelli, M.; Sato, M.; Enemark, J. H.; Kroneck, P. M. H.; Sulger, K. *Inorg. Chem.* **1983**, *22*, 3065.

(54) Sellmann, D.; Prechtel, W.; Knoch, F.; Moll, M. *Z. Naturforsch.* **1992**, *47b*, 1411.

(55) Sellmann, D.; Emig, S.; Heinemann, F. W.; Knoch, F. *Angew. Chem.* **1997**, *109*, 1250; *Angew. Chem., Int. Ed. Engl.* **1997**, *36*, 1201.

(56) Sellmann, D.; Emig, S.; Heinemann, F. W. *Angew. Chem.* **1997**, *109*, 1808; *Angew. Chem., Int. Ed. Engl.* **1997**, *36*, 1734.

(57) Baldas, J.; Boas, J.; Bonnyman, J.; Mackay, M. F.; Williams, G. A. *Aust. J. Chem.* **1982**, *35*, 2413.

(58) Yamaouchi, K.; Enemark, J. H. *Inorg. Chem.* **1978**, *17*, 1981.

(59) Yamaouchi, K.; Enemark, J. H. *Inorg. Chem.* **1978**, *17*, 2911.

(60) Sellmann, D.; Ruf, R.; Knoch, F.; Moll, M. *Inorg. Chem.* **1995**, *34*, 4745.

(61) (a) Vogel, S.; Huttner, G.; Zsolnai, L. *Z. Naturforsch.* **1993**, *48b*, 641. (b) Tong, Y.-X.; Kang, B.-S.; Su, C.-Y.; Yu, X.-L.; Chen, X.-M. *J. Chem. Crystallogr.* **1998**, *28*, 635.

(62) Liaw, W.-F.; Lee, Ch.-M.; Lee, G.-H.; Peng, S.-M. *Inorg. Chem.* **1998**, *37*, 6396.

(63) Danopoulos, A. A.; Wong, A. C. C.; Wilkinson, G.; Hursthouse, M. B.; Hussain, B. *J. Chem. Soc., Dalton Trans.* **1990**, 315.

(64) Kawamoto, T.; Nagasawa, I.; Kuma, H.; Kushi, Y. *Inorg. Chim. Acta* **1997**, *265*, 163.

(65) Kawamoto, T.; Kuma, H.; Kushi, Y. *Bull. Chem. Soc. Jpn.* **1997**, *70*, 1599.

(66) Henkel, G.; Krebs, B.; Schmidt, W. *Angew. Chem.* **1992**, *104*, 1380; *Angew. Chem., Int. Ed. Engl.* **1992**, *31*, 1366.

(67) Darensbourg, D. J.; Draper, J. D.; Frost, B. J.; Reibenspies, J. H. *Inorg. Chem.* **1999**, *38*, 4705.

(68) Liaw, W.-F.; Lee, N.-H.; Chen, C.-H.; Lee, C.-M.; Lee, G.-H.; Peng, S.-M. *J. Am. Chem. Soc.* **2000**, *122*, 488.

(69) Kawamoto, T.; Kushi, Y. *Chem. Lett.* **1992**, 893.

(70) Miller, E. J.; Rheingold, A. L.; Brill, T. B. *J. Organomet. Chem.* **1985**, *282*, 399.

(71) (a) Pierpont, C. G.; Downs, H. H. *J. Am. Chem. Soc.* **1976**, *98*, 4834. (b) Buchanan, R. M.; Kessel, S. L.; Downs, H. H.; Pierpont, C. G.; Hendrickson, D. N. *J. Am. Chem. Soc.* **1978**, *100*, 7894. (c) Sofen, S. R.; Ware, D. C.; Cooper, S. R.; Raymond, K. N. *Inorg. Chem.* **1979**, *18*, 234. (d) Downs, H. H.; Buchanan, R. M.; Pierpont, C. G. *Inorg. Chem.* **1979**, *18*, 1736. (e) Lange, C. W.; Conklin, B. J.; Pierpont, C. G. *Inorg. Chem.* **1994**, *33*, 1276.

(72) Kirmse, R.; Stach, J.; Spies, H. *Inorg. Chim. Acta* **1980**, *45*, L251−L253.

spectrum. According to our coupling scheme an Os(III) (low-spin d^5) can couple antiferromagnetically with only one ligand radical. The remaining two ligand radicals must then couple antiferromagnetically.

It is interesting that Enemark et al.[59] have been able to structurally characterize the complex [Mo(abt)$_2$(dithiocarbamato)] ($S_t = 1/2$) which they describe as Mo(V) d^1 complex. Note that in this complex one of the three noninnocent abt−(1-) ligands in [Mo(abt)$_3$] is formally replaced by an *S,S*-coordinated innocent dithiocarbamato(1-) ligand. Therefore, we propose that this complex, in fact, is also a Mo(III)d^3 species where antiferromagnetic coupling to *two o-iminothionesemiquinonate* radicals generates the observed metal-centered $S_t = 1/2$ ground state.

Huttner et al.[61a] have reported a five-coordinate, diamagnetic [(tripod)Co^{III}(abt)]$^+$ complex where "tripod" represents the neutral phosphane ligand CH$_3$C(CH$_2$PPh$_2$)$_3$. The geometric details of the abt ligand very clearly allow its assignment as monoanionic radical. Therefore, we reformulate this compound as [(tripod)Co^{II}(*o*-iminothionesemiquinonate)]$^+$ where a low-spin Co^{II} d^7 ($S_{Co} = 1/2$) is coupled antiferromagnetically to a ligand radical yielding the observed $S_t = 0$ ground state. A very similar structure has been reported for "[Co^{II}(*o*-SC$_6$H$_4$NH$_2$)-{P(OMe)$_3$}$_3$]PF$_6$"[61b] where the authors claim the presence of an *N,S*-coordinated diamagnetic aromatic aminothiophenolate-(1-), *o*-SC$_6$H$_4$NH$_2^-$, ligand, but their crystal structure clearly shows the presence of an abt^{1-} π-radical anion of type D in agreement with the fact that in the IR spectrum a single ν(N−H) stretching mode at 3332 cm^{-1} has been reported. Consequently, this compound should be reformulated as [Co^{II}(*o*-SC$_6$H$_4$NH−){P(OMe)$_3$}$_3$]PF$_6$ which should possess an $S = 0$ ground state, whereas the original formulation requires an $S = 1/2$ ground state which has not been experimentally established by these authors.

Sellmann and co-workers have in recent years extensively studied the coordination chemistry of 1,2-ethanediamine-*N,N'*-bis(2-benzenethiol), H$_2$(L^1), with iron and ruthenium. They have reported an extremely interesting series of five-coordinate mononuclear species where the ligand was assigned an oxidation level as in type C containing two N-deprotonated dianionic *o*-amidophenolate(2-) entities in each case: [Fe^{IV}(L^1)(PR$_3$)] ($S_t = 1$),[6] [Ru^{IV}(L^1)(PR$_3$)] ($S_t = 0$)[60] and even [Fe^V(L^1)I] ($S_t = 1/2$).[56] Each of these compounds has been structurally and spectroscopically carefully characterized. Inspection of the structural data immediately implies that in each of the above cases the *N,S*-coordinated ligand is of type D, that is, *o*-iminothionesemiquinonate(1-), rendering the tetradentate ligand a dianionic diradical: In all cases the S−C$_{phenyl}$ *and* the N−C$_{phenyl}$ bonds are rather short at ∼1.73 and ∼1.35 Å, respectively, and, in addition, in all structures the six-membered phenyl rings display distinctly quinoid character. Thus, we propose that these compounds should be considered to be [Fe^{II}(L$^{1\bullet\bullet}$)(PR$_3$)] ($S_t = 1$), [Ru^{II}(L$^{1\bullet\bullet}$)(PR$_3$)] ($S_t = 0$), and [Fe^{III}(L$^{1\bullet\bullet}$)I] ($S_t = 1/2$) species.[3c] This is unambiguously established in this work by a spin-Hamiltonian analysis of the applied field Mössbauer spectrum for [Fe^{II}(L$^{1\bullet\bullet}$)(PR$_3$)] and, previously, for [Fe^{III}(L$^{1\bullet\bullet}$)I].[3d] For the latter species we have shown that the structural and all spectroscopic data (EPR, UV−vis, Mössbauer) are compatible with a description of the electronic structure of this species as intermediate spin iron(III) ($S_{Fe} = 3/2$) coupled intramolecularly to two *o*-iminothionesemiquinonato(1-) radicals.[3d] This notion has been reinforced by the synthesis and structural and spectroscopic characterization of the completely analogous compound [Fe^{III}(L$^{2\bullet}$)$_2$I] ($S = 1/2$) where L$^{2\bullet}$ represents the *O,N*-

coordinated, monoanionic, sulfur-free *N*-phenyl-*o*-iminobenzo-semiquinonate(1-) π-radical.[3d]

We would now like to draw attention to some five-coordinate organometallic and carbonyl compounds containing, according to the authors, a single *N,S*-coordinated *o*-amidothiophenolate-(2-) ligand: [Cp*Co(abt)],[70] [PPN][Fe(CO)$_2$(CN)(abt)][68] and [PPN][Mn(CO)$_3$(abt)],[62] and [PPN]$_2$[W(CO)$_3$(abt)][67] all of which are diamagnetic ($S_t = 0$), and room-temperature X-ray structures of good quality have been reported. The C−S and N−C bond distances are observed in the narrow range 1.714−1.732 and 1.364−1.376 Å, respectively, and all coordinated ligands display some quinoid character of the phenyl ring, although not in all cases at the 3σ level of confidence. According to the above analysis the coordinated abt ligands belong to type D; they can be considered to be radical monoanions. This would lead us to ascribe formal oxidation states to the metal ions as follows: low-spin cobalt(II) in [Cp*Co(abt$^\bullet$)] and −I in [W(CO)$_3$(abt$^\bullet$)]$^{2-}$, 0 in [Mn(CO)$_3$(abt$^\bullet$)]$^-$ and +I in [Fe(CO)$_2$(CN)(abt$^\bullet$)]$^-$. In all cases there is then an unpaired electron at the metal center (antiferromagnetically coupled to a ligand radical) which may well be delocalized over the Cp-metal and carbonylmetal fragments as was shown recently to be the case by Holm et al.[73] for the redox series [M(CO)$_2$(S$_2$C$_2$Me$_2$)$_2$]$^{0/1-/2-}$ (M = Mo, W). Clearly, in these cases the concept of *localized* ligand- *and* metal-centered oxidation states is of limited value but the noninnocent nature of the *N,S*-coordinated abt ligand is again clearly established.

In the following, we discuss the electronic structures of the paramagnetic monocations [**1a/1b**]$^+$ and [**3a**]$^+$ in comparison with their corresponding−also paramagnetic−monoanions [**1a/1b**]$^-$ and [**3a**]$^-$. Significantly, the EPR spectra of the monocations immediately rule out the presence of Ni(III) or Pt(III) with a (d$_{z^2}$)^1 ground state.[74] The EPR spectra of genuine square-planar (amidate−thiolate)nickel(III) complexes have been analyzed by Holm et al.[75] Their spectra display nearly axial symmetry, have $g_{iso} > 2.1$, and display large anisotropies with $g_\perp > g_{||}$ and $g_{||} = 2$ consistent with a σ^*(d$_{z^2}$) ground state. In contrast, the spectra of [**1a/1b**]$^+$ and [**3a**]$^+$ have g_{iso} values at 2.0014 and 2.0073, respectively, and very small anisotropies in accord with the presence of a coordinated (L^{ISQ})$^{1-}$ π-radical. The small hfc constant of A_{iso}(^{195}Pt) of 9.5 G observed for [**3a**]$^+$ is clearly not consistent with a genuine Pt(III) complex. Thus, we propose ligand- and metal-centered oxidation levels for these monocations as [M^{II}(L^{ISQ})(L^{IBQ})]$^+$. As pointed out above, this is also in agreement with the observed electronic spectra where strong intraligand CT bands of a coordinated (L^{IBQ}) ligand in the range 500−650 nm are observed. These data lend support to the notion that these monocations contain localized oxidation levels of the metal ions and ligands, namely a semiquinonate-(1-), as well as a neutral benzoquinone-type ligand, and a d^8-configurated divalent metal ion.

The EPR spectra of the monoanions [**1a/1b**]$^-$ and [**3a**]$^-$ are remarkably different from those of the above monocations. They display a significantly larger g anisotropy and the g_{iso} values are significantly larger than 2.00. For genuine tetradentate (square-planar) monovalent Ni^I species in an N$_4$-macrocyclic environment the unpaired electron resides in the (d$_{x^2-y^2}$) orbital and all g values are >2, and $g_{||} > g_\perp$.[76] This is apparently also

(73) Fomitchev, D. V.; Lim, B. S.; Holm, R. H. *Inorg. Chem.* **2001**, *40*, 645.

(74) For recent explanatory reviews of Ni(I), (III) EPR spectra, see: Coyle, C. L.; Stiefel, E. I.; Salerno, J. C.; Eidsness, M. K.; Sullivan, R. J.; Scott, R. A. In *Bioinorganic Chemistry of Nickel*; Lancaster, J. R., Jr., Ed.; VCH Publishers: New York, 1988; pp 1, 53, 73.

(75) Krüger, H.-J.; Peng, G.; Holm, R. H. *Inorg. Chem.* **1991**, *30*, 734.

the case for the spectrum [**1a/1b**]⁻. In addition, the spectrum of [**3a**]⁻ displays a large *g* anisotropy and a very large hfc constant $A_{iso}(^{195}Pt)$ of 109 G supporting the view that the unpaired electron resides at least to some extent in a metal d-orbital. A *localized* description as $[M^I(L^{ISQ})_2]^-$ is nevertheless inappropriate since we would expect the electronic spectra of both the neutral $[M(L^{ISQ})_2]$ *and* the monoanionic $[M^I(L^{ISQ})_2]^-$ species to display the same (or very similar) intense ($\epsilon \approx 10^4$ L mol⁻¹ cm⁻¹) ligand-to-ligand CT band at ∼850 nm which is clearly not the case. The electronic spectra of [**1a/1b**]⁻ and [**3a**]⁻ do show the presence of $(L^{ISQ})^{1-}$ ligands, and a description as $[M^{II}(L^{AP}-H)(L^{ISQ})]^-$ would be in accord. In a valence bond description the two structures could represent resonance hybrids:

$$[M^I(L^{ISQ})_2]^- \leftrightarrow [M^{II}(L^{AP}-H)(L^{ISQ})]^-$$

Interestingly, the room-temperature crystal structure of [AsPh₄]-[Ni(*o*-C₆H₄(NH)S)₂] has been reported by Peng et al.[77] The structure is of low quality, but three observations are remarkable: (i) the two *N,S*-coordinated ligands of a monoanion are related by a crystallographically imposed inversion center, they are equivalent; (ii) the C−S and C−N distances are short at 1.72 ± 0.02 and 1.35 ± 0.03 Å indicating the presence of the *o*-iminothionesemiquinonato(1-) oxidation level at the ligands but the phenyl rings do *not* show the quinoid type structure; the six C−C distances are equivalent within the very large error limits of 0.03−0.04 Å (3σ); (iii) the average Ni−S bond length at 2.19 ± 0.01 Å and the corresponding Ni−N distance at 1.81 ± 0.02 Å are slightly and barely significantly longer than those in the neutral complex **1a** at 2.151 ± 0.003 Å and 1.792 ± 0.01 Å, respectively. This may indicate the presence of some Niᴵ character in the monoanion. On the other hand, Sellmann et al.[78] have structurally characterized the square-planar monoanion [Ni('N₂S₂')]⁻ in its tetraphenylarsonium salt. The structural data, although of rather low quality, appear to indicate the presence of genuine Niᴵᴵᴵ (d⁷) and a tetraanionic ligand 1,2-ethanediamido-*N,N*-bis(2-benzenethiolate)(4-) since the observed average C−S and C−N bond distances at 1.795-(30) and 1.39(3) Å are typical for a type C structure (Table 6). Unfortunately, further spectroscopic characterizations, in particular its EPR spectrum, have not been reported.

The early crystal structure of [Et₄N][Ni(H₂dma)][79] where H₂dma is the 1,2-dimethyl substituted analogue of the "N₂S₂" ligand above is more in agreement with type D with short C−S and C−N bonds at 1.71(2) and 1.365(20) Å, respectively. Its reported EPR and UV−vis spectra are very similar to those reported here for [**1a/1b**]⁻. In conclusion, the present data on [**1a/1b**]⁻ and Peng's structure are fully consistent with those reported for [Ni(H₂dma)]⁻ [79] for which the authors describe its electronic structure as follows: "The four-coordinate, planar NiN₂S₂ structure is in good agreement with the coordinated radical formulation [Niᴵᴵ(H₂dma³⁻)]⁻, in which the ligand is partially oxidized and the metal has the d⁸ configuration characteristic of planar coordination. It is difficult to reconcile

the structural data with *either* a Ni(I) or a Ni(III) formulation." It is then rather difficult to understand the geometric and electronic structure differences between these and Sellmann's complex.[78] A structural reinvestigation of all of these complexes at cryogenic temperatures and more spectroscopic data are clearly necessary to resolve this problem experimentally.

Conclusions

We have shown in this study that *N,S*-coordinated *o*-aminothiophenolato ligands are noninnocent ligands in the sense that they exist in three different oxidation levels in coordination compounds: (i) aromatic mono- and dianions (depending on the degree of protonation (amine or amide) or substitution at the amine functionality); (ii) *o*-iminothionebenzosemiquinonates-(1-) π-radicals; (iii) the *o*-iminothionequinone level has as yet not been structurally characterized in a complex, but its electronic spectral characteristics have been established by two intense π−π* CT bands in the visible at ∼640 and 560 nm.

In general, the structural parameters for each level A to D given in Table 6 do not depend greatly on the nature of the transition metal ion to which they are bound or the number of such ligands in a given compound, or their arrangement relative to each other (*cis*, or *trans* in square-planar complexes or in octahedral species).

The unpaired electron spin of an *N,S*-coordinated *o*-imino-thionesemiquinonate radical couples invariably intramolecularly and strongly to the unpaired electron spin of an incompletely filled t₂g subshell of a given transition metal ion, $|J| \gg 400$ cm⁻¹. If the t₂g subshell is filled as in low-spin Fe(II) or Ru(II) two such radicals can couple ferro- or antiferromagnetically.

While the above analysis of the C−S and C−N bond distances in *N,S*-coordinated *o*-aminothiophenolate and its oxidized radical form as obtained from high-quality crystallography is compelling (at least for Werner-type complexes), we emphasize that the actual electronic structure of such a species can only be reliably established in conjunction with other spectroscopic techniques such as, for example, electron spin resonance, UV−vis absorption and Mössbauer spectroscopy, magnetochemistry, and X-ray absorption near edge (XANES) spectroscopy. Finally, state of the art density functional calculations should also shed light on the electron density distributions in such compounds. In a forthcoming paper we will report such a study on the neutral complexes [Niᴵᴵ(X−C₆H₄−Y)₂] where X = Y = O, NH, S, and X =NH and Y = O, S. We show that all of the complexes are to be described as singlet diradicals. In particular, the singlet−triplet energy gap in [Niᴵᴵ(HN−C₆H₄−S)₂] is of the order of 4000 cm⁻¹, whereas it is ∼900 cm⁻¹ in [Niᴵᴵ(O−C₆H₄−O)₂], rendering both species diamagnetic at 300 K.

Supporting Information Available: Figure S1, displaying the dinuclear, supramolecular assembly in **2**, and Tables of crystallographic structure refinement data, atom coordinates, bond lengths and angles, anisotropic thermal parameters of non-hydrogen atoms, and calculated positional parameters of H atom for complexes **1a**·dmf, **2**, and **3a**·CH₂Cl₂ (PDF). This material is available free of charge via the Internet at http://pubs.acs.org.

JA011155P

(76) (a) Lovecchio, F. V.; Gore, E. S.; Busch, D. H. *J. Am. Chem. Soc.* **1974**, *96*, 3109. (b) Busch, D. H. *Acc. Chem. Res.* **1978**, *11*, 392.

(77) Liaw, M.-C.; Lee, G.-H.; Peng, S.-M. *Bull Inst. Chem., Acad. Sin.* **1993**, *40*, 23.

(78) Sellmann, D.; Prechtel, W.; Knoch, F.; Moll, M. *Z. Naturforsch.* **1992**, *47b*, 1411.

(79) Dori, Z.; Eisenberg, R.; Stiefel, E. I.; Gray, H. B. *J. Am. Chem. Soc.* **1970**, *92*, 1506.